Available online at www.sciencedirect.com
SCIENCE DIRECT
Tetrahedron 62 (2006) 4749–4755
Tetrahedron

Synthesis of end-functionalized π-conjugated porphyrin oligomers

Hiroaki Ozawa,[a,b] Masahiro Kawao,[a,b] Hirofumi Tanaka[a,b,c] and Takuji Ogawa[a,b,c,*]

[a]*Research Center for Molecular-Scale Nanoscience, Institute for Molecular Science, 5-1 Higashiyama, Myodaiji, Okazaki 444-8787, Japan*
[b]*Graduate University for Advanced Studies, Hayama, Miura 240-0193, Japan*
[c]*Core Research for Evolutional Science and Technology (CREST) of Japan Science and Technology Agency (JST), Hon-Machi 4-1-8, Kawaguchi, Saitama 332-0012, Japan*

Received 26 January 2006; revised 9 March 2006; accepted 10 March 2006
Available online 3 April 2006

Abstract—4-(*S*-Acetylthiomethyl)phenyl- and pyrenyl-functionalized π-conjugated porphyrin oligomers were synthesized. The distribution of the length of the oligomers could be controlled by changing the ratio of the starting porphyrin to the capping molecules. Oligomers from dimers to heptamers were isolated using size exclusion chromatography. The spectroscopic properties of these oligomers were measured to determine the influences of the number of porphyrin units and capping molecules on the absorption and emission spectra.

1. Introduction

Molecular electronics is a fascinating area of fundamental research with the potential for many future applications.[1–4] In recent years, studies on the conductance of single or small numbers of molecules were reported with intriguing results, exhibiting such interesting properties as switching,[5,6] the Coulomb-blockade phenomenon,[7–9] field-effect transistor,[7–10] and the Kondo effect.[9,11] As an extension of these studies, the fabrication of larger nanostructures constructed from organic molecules as the functional moieties and conductive nanomaterials as the electron transport portion has been recognized as an important issue for future nanodevices (Fig. 1). Metal nanoparticles,[12,13] metal nanorods,[14] and carbon nanotubes[15,16] are promising candidates for conductive nanomaterials. In order to construct such nanocomposites made from conductive materials and organic molecules, functional groups are required to couple these moieties together. Mercapto or *S*-acetylthio groups are known to be good coupling groups to metals,[17] and aromatic hydrocarbons such as pyrene are known to adsorb to the surface of carbon nanotubes efficiently through π–π interactions.[18] For the purpose of constructing such nanocomposites[19–22] using a series of porphyrin oligomers as the organic portion,

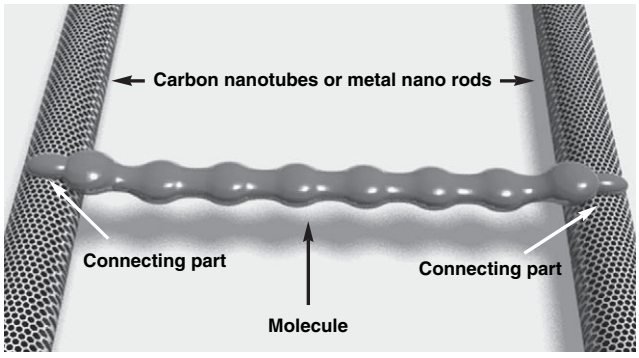

Figure 1. Schematic diagram of nanostructures consisting end-functionalized oligomers and conductive materials.

we synthesized a series of end-functionalized π-conjugated porphyrin oligomers. One series (**1a**–**g**) contains 1-[4-(*S*-acetylthiomethyl)phenyl]ethynyl groups and another series (**2a**–**g**) bears 2-pyrenylethynyl groups at the end of the molecules. Systematic spectroscopic studies of this series of oligomers were performed to study their electronic properties, especially to clarify the effects of the end-functional groups on the main π-conjugated electronic systems.

2. Results and discussion

2.1. Synthesis

End-functionalized porphyrin oligomers **1a**–**g** and **2a**–**g** were synthesized by the synthetic route shown in Scheme 1.

Supplementary data associated with this article can be found in the online version at doi:10.1016/j.tet.2006.03.031.
Keywords: Porphyrin oligomers; Spectroscopic properties; 4-(*S*-Acetylthiomethyl)phenyl; Pyrenyl.
* Corresponding author. Tel.: +81 564 59 5536; fax: +81 564 59 5535; e-mail: ogawat@ims.ac.jp

0040–4020/$ - see front matter © 2006 Elsevier Ltd. All rights reserved.
doi:10.1016/j.tet.2006.03.031

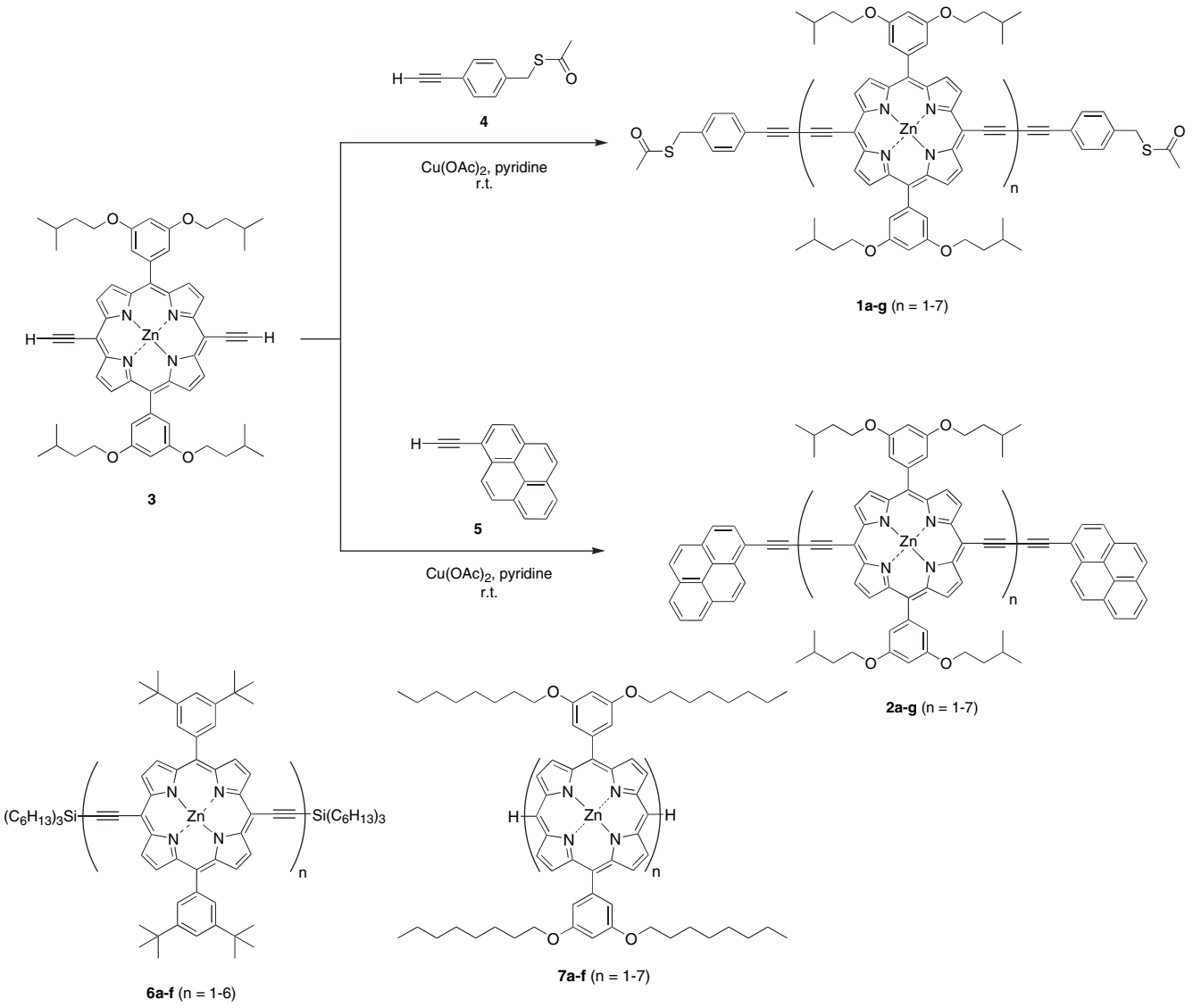

Scheme 1. Synthesis of end-functionalized porphyrin oligomers (**1a–g** and **2a–g**) and structures of silicon-functionalized (**6a–f**) and meso–meso linked (**7a–f**) porphyrin oligomers.

Functional alkynes **4** or **5** were used as the capping molecules. The oxidative coupling reaction of compound **3** and these capping molecules via copper catalysis gave a series of oligomers. The porphyrin-containing products were first purified by gel permeation chromatography (GPC) and further isolated by recycling high performance liquid chromatography GPC (HPLC–GPC). The details of the synthesis and isolation are presented in Section 4. The purities of these oligomers were confirmed by ^{1}H NMR, MALDI-TOF-MS, and analytical GPC (see Section 4 and Supporting information).

The distribution of oligomers could be controlled by changing the ratio of compound **3** to the capping molecules (**4** or **5**), as depicted in Figure 2. When the compound ratio of **3** to **4** was 1:2 (entry 1), the main product was monomer. When the ratio was 5:2 (entry 2), the major products ranged from tetramer to hexamer. When the ratio was 10:1 (entry 3), the distribution peak of oligomers centered on a decamer.

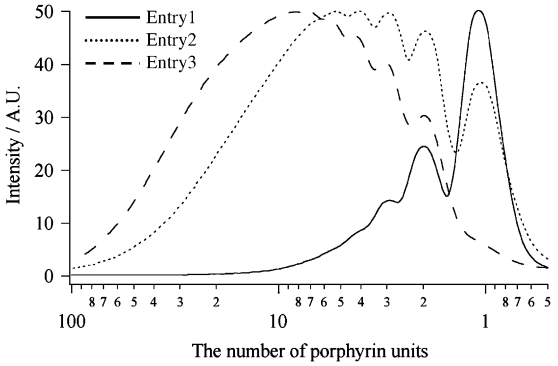

Figure 2. Analytical GPC data of porphyrin oligomers prepared by changing the compound ratio of **3** to **4**. The compound ratios of **3** to **4** were 1:2, 5:2, and 10:1 for entries 1, 2, and 3, respectively.

2.2. UV and fluorescence spectra of the oligomers

UV–vis absorption spectra of end-functionalized porphyrin oligomers **1a–g** and **2a–g** in THF are shown in Figure 3a

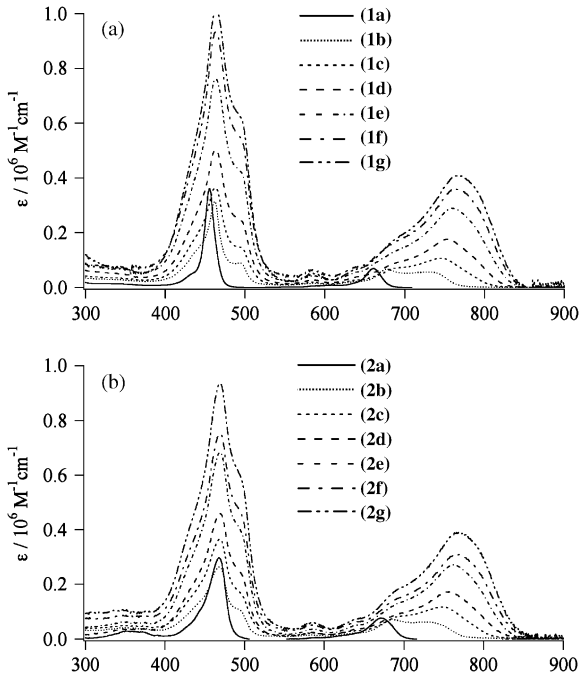

Figure 3. UV–vis spectra of: (a) acetylthiomethylbenzene-capped porphyrin oligomers **1a**–**g** and (b) pyrene-capped porphyrin oligomers **2a**–**g** measured in THF.

and b, respectively, and the peak wavelengths λ_{max} are tabulated in Table 1. The Soret peaks of the porphyrin oligomers were gradually red-shifted as the size of the oligomer increased. The Q bands were also red-shifted and intensified with increasing porphyrin units, indicating a high degree of conjugation. The Soret and Q band absorption maxima were dependent on the end-functional groups. Oligomers **2a**–**g** with pyrene end groups showed longer wavelength absorption compared to the corresponding oligomers **1a**–**g** with 4-(*S*-acetylthiomethyl)phenyl groups. The absorption coefficients of these oligomers became larger with the increasing number of porphyrin units. The absorption coefficients increased with a linear relationship to the number of porphyrin units with the exception of the monomer.

Table 1. The absorption λ_{max} (in THF), emission λ_{max} (in THF), and fluorescence quantum yield of porphyrin oligomers **1a**–**g** and **2a**–**g**

Porphyrin oligomer	Absorption λ_{max}/nm	Emission[a] λ_{max}/nm	Φ_F[b]
1a	455, 661	674	0.09
1b	462, 493, 583, 677, 725	750	0.10
1c	463, 583, 744	780	0.07
1d	463, 584, 752	792	0.08
1e	463, 585, 758	800	0.07
1f	463, 585, 764	804	0.07
1g	463, 585, 768	808	0.07
2a	467, 671	688	0.09
2b	468, 583, 685, 730	758	0.12
2c	468, 584, 747	782	0.09
2d	469, 584, 756	796	0.09
2e	469, 584, 762	802	0.07
2f	469, 584, 766	806	0.07
2g	469, 583, 769	808	0.07

[a] Emission spectra were taken for excitation at Soret band.
[b] Tetraphenylporphyrin in benzene (TPP, Φ_F=0.11) was used as a standard.[25]

Fluorescence data of these oligomers are also depicted in Table 1. These emission spectra show no dependency on excitation wavelength and the excitation spectra were coincident with the absorption spectra, which confirms that these emissions are not from any impurities. From the absorption and emission data, HOMO–LUMO energy gaps E_g were estimated. The values of E_g are plotted against the reciprocal of the number of porphyrin units ($1/N$) in Figure 4. These plots are linear, with no sign of saturation. The E_g value for **1a** obtained from absorption data (1.88 eV) is 0.03 eV larger than that for **2a** (1.85 eV), which is reasonably explained by the differences in the degree of resonance of the capping moieties. The E_g ($N=\infty$) values obtained from the intercepts for a series of **1** and **2** were coincident to be 1.57 eV from the absorption data and 1.48 eV from the emission data. This means that though the optical properties of the monomer were highly influenced by the capping molecules, the effect decreased with an increasing number of porphyrin units. Therefore, we can conclude that the optical properties of long oligomers were minimally influenced by the end-capping moieties. The reported E_g ($N=\infty$) obtained from the emission of a series of **6** was 1.34 eV, which is significantly lower than the values obtained for **1** and **2**.[23] This can be attributed to a difference in the measurement conditions. Because of the low solubility of **6**, a small amount of pyridine was added to the solution. Most likely, the pyridine molecules coordinated to the zinc metal of each porphyrin unit, lowering the E_g values by the extended resonance.[24]

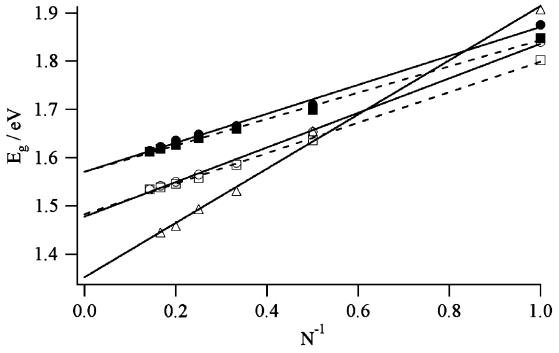

Figure 4. Plot of optical band gap energy E_g against the reciprocal of the number of porphyrin units $1/N$ for (●) **1a**–**g** (absorption), (■) **2a**–**g** (absorption), (○) **1a**–**g** (emission), (□) **2a**–**g** (emission), and (△) **6a**–**f** with pyridine (emission).[23]

The relative fluorescence quantum yields were determined using tetraphenylporphyrin (H_2TPP) as the standard (Φ_F=0.11).[25] The quantum yield of the monomers (**1a** and **2a**) was 0.09, and this decreased gradually with the increase in the number of porphyrin units (Table 1 and Fig. 5). The results shown are in sharp contrast with a report for meso–meso linked porphyrin oligomer **7**.[26–28] In the latter compounds, the quantum yield of the fluorescence for the monomer was 0.022 and increased as the number of porphyrin units increased in the arrays. This phenomenon is attributed to the increase of the rotational diffusion time by the anisotropic elongation of the molecules. As the rotational diffusion time increased, the natural radiative lifetime decreased, and consequently the fluorescence quantum yield increased. The reason for the difference between **7** and **1** or **2** is not clear at present, but the degree of conjugation between porphyrin moieties might be responsible.

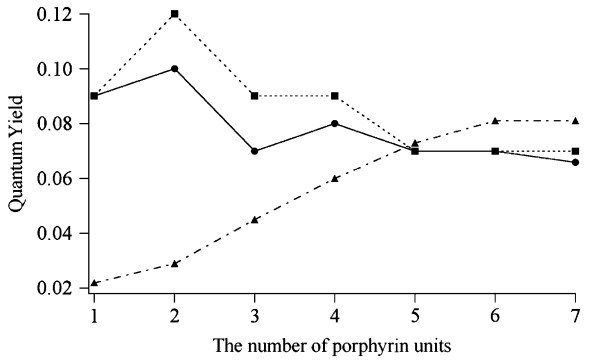

Figure 5. Plots of quantum yield versus the number of porphyrin units for (●) **1a–g**, (■) **2a–g**, and (▲) **7a–g**.[26]

3. Conclusion

We report the preparation and isolation of a series of end-functionalized porphyrin oligomers by a simple coupling reaction. The distribution of oligomers can be controlled by the ratio of porphyrin derivative to capping molecules. UV–vis absorption and fluorescence spectra of the monomers were affected by the capping groups; however, the effect decreased as the number of porphyrin units increased. The fluorescence quantum yield decreased as the number of porphyrin units increased, which showed a sharp contrast with a series of meso–meso coupled porphyrin oligomers. Construction of nanostructures consisting these end-functionalized molecules and metal particles or carbon nanotubes is now in progress.

4. Experimental

4.1. General

Compounds **3**,[29,30] **4**,[31] and **5**[32] were prepared according to published literature procedures. All solvents and reagents were of commercial reagent grade and were used without further purification except where noted. ^{1}H NMR spectra were recorded on a JEOL JNM-LA400 spectrometer and chemical shifts were reported in the delta scale relative to an internal standard of TMS (δ=0.00). Spectroscopic grade tetrahydrofuran (THF) and benzene were used as solvents for all spectroscopic measurements. UV–vis absorption spectra were recorded on a Shimadzu UV-3150 spectrophotometer. Fluorescence measurements were carried out with a JASCO FP-6600 spectrometer. Infrared spectra were obtained on a JASCO FT/IR-460plus. All MALDI-TOF-MS spectra were obtained using an Applied Biosystem Voyager DE-STR with 9-nitroanthracene and dithranol as the matrices. Analytical gel permeation chromatography (GPC) was carried out using Shimadzu LC-6A equipped with a diode array detector (MD-2015, JASCO) and two serially connected GPC KF-804L columns. THF was used as the eluent and the flow rate in all experiments was 1.0 mL/min. Recycling preparative GPC–HPLC was carried out on JAI LC-908 using serially connected preparative scale JAIGEL-2.5H, 3H, and 4H columns. Preliminary separation of the oligomers was performed by open column chromatography-GPC using Bio-Beads S-X1 (BioRad) and THF as the eluent.

4.2. General procedure

4.2.1. Preparation and isolation of 4-(*S*-acetylthiomethyl)phenyl functionalized porphyrin oligomers. In a round-bottomed flask, compounds **3** (52 mg, 57 μmol), **4** (11 mg, 57 μmol), and $Cu(OAc)_2$ (31 mg, 170 μmol) were dissolved in 5 mL of pyridine and the mixture was stirred at room temperature for 12 h. Water was added to the reaction and the resulting precipitate was filtered and washed with methanol. The precipitate was dissolved in THF and passed through an open column chromatograph using Bio-Beads S-X1 (BioRad) to obtain a mixture of the products containing porphyrin oligomers. These oligomers were further isolated by recycling GPC–HPLC to give the following: **1a** (5 mg, 6%), **1b** (19 mg, 31%), **1c** (8 mg, 14%), **1d** (6 mg, 10%), **1e** (5 mg, 8%), **1f** (3 mg, 5%), **1g** (1 mg, 2%), and larger oligomers (6 mg). The purity of each homologue was checked by the following analyses. The ^{1}H NMR spectrum of each sample showed consistent integrations for all the resonances, and no evidence of impurities was observed (Figs. 1S–7S). With the MALDI-TOF-MS spectra, no other homologues were detected for each isolated product (Fig. 15S). We conducted analytical GPC analyses of each product with simultaneous measurements of the absorption spectra using a diode array detector (Figs. 17S–20S). All the isolated oligomers showed a single peak clearly distinguishable from other oligomers by its retention time and absorption spectrum (Fig. 25S).

4.2.2. Control of product distribution by changing the ratio of 3 to 4 (entry 1). In a round-bottomed flask, **3** (52 mg, 57 μmol), **4** (225 mg, 118 μmol), and $Cu(OAc)_2$ (30 mg, 167 μmol) were dissolved in 5 mL of pyridine and the mixture was stirred at room temperature for 12 h. Water was added to the reaction and the resulting precipitate was filtered and washed with methanol. The precipitate was dissolved in THF and passed through an open column chromatograph using Bio-Beads S-X1 (BioRad) to obtain a mixture of the products containing porphyrin oligomers (55 mg). The distribution of the products was determined by analytical GPC of the mixture.

4.2.3. Control of product distribution by changing the ratio of 3 to 4 (entry 2). In a round-bottomed flask, **3** (51 mg, 55 μmol), **4** (4 mg, 20 μmol), and $Cu(OAc)_2$ (30 mg, 170 μmol) were dissolved in 5 mL of pyridine and the mixture was stirred at room temperature for 12 h. Water was added to the reaction and the resulting precipitate was filtered and washed with methanol. The precipitate was dissolved in THF and passed through an open column chromatograph using Bio-Beads S-X1 (BioRad) to obtain a mixture of the products containing porphyrin oligomers (42 mg). The distribution of the products was determined by analytical GPC of the mixture.

4.2.4. Control of product distribution by changing the ratio of 3 to 4 (entry 3). In a round-bottomed flask, **3** (51 mg, 56 μmol), a THF solution of **4** (52 μL solution of 10 mg/mL concentration, 2.8 μmol) and $Cu(OAc)_2$ (30 mg, 167 μmol) was dissolved in 5 mL of pyridine and the mixture was stirred at room temperature for 12 h. Water was added to the reaction and the resulting precipitate was filtered and washed with methanol. The precipitate was

dissolved in THF and passed through an open column chromatograph using Bio-Beads S-X1 (BioRad) to obtain a mixture of the products containing porphyrin oligomers (36 mg). The distribution of the products was determined by analytical GPC of the mixture.

4.2.5. Preparation and isolation of pyrenyl-functionalized porphyrin oligomers. In a round-bottomed flask, **3** (51 mg, 56 μmol), **5** (13 mg, 56 μmol), and $Cu(OAc)_2$ (30 mg, 167 μmol) were dissolved in 5 mL of pyridine and the mixture was stirred at room temperature for 12 h. Water was added to the reaction and the resulting precipitate was filtered, washed with methanol, and roughly purified by open column chromatography-GPC. The oligomers were isolated by a recycling GPC–HPLC to give the following: **2a** (13 mg, 18%), **2b** (14 mg, 23%), **2c** (10 mg, 16%), **2d** (7 mg, 12%), **2e** (4 mg, 6%), **2f** (3 mg, 6%), **2g** (2 mg, 4%), and larger oligomers (4 mg). The purity of each homologue was checked by the following analyses. The ^{1}H NMR spectra of each sample showed consistent integrations for all the resonances, and no evidence of impurities was observed (Figs. 8S–14S). With the MALDI-TOF-MS spectra, no other homologues were detected for each isolated product (Fig. 16S). We conducted analytical GPC analyses of each product with simultaneous measurements of the absorption spectra using a diode array detector (Figs. 21S–24S). All the isolated oligomers showed a single peak clearly distinguishable from other oligomers by its retention time and absorption spectrum (Fig. 26S).

4.2.5.1. Compound 1a. ^{1}H NMR (400 MHz, d_8-THF) δ 9.57 (d, J=5 Hz, 4H, β-pyrrole), 8.96 (d, J=5 Hz, 4H, β-pyrrole), 7.65 (d, J=8.3 Hz, 4H, Ar), 7.40 (d, J=8.3 Hz, 4H, Ar), 7.32 (d, J=2 Hz, 4H, Ar), 6.95 (t, J=2 Hz, 2H, Ar), 4.21 (t, J=7 Hz, 8H, OCH_2), 4.18 (s, 4H, SCH_2Ph), 2.34 (s, 6H, $C(O)CH_3$), 1.92 (sext, J=7 Hz, 8H, CH_2), 1.77 (m, J=7 Hz, 4H, CH), 1.00 (d, J=7 Hz, 24H, CH_3). HRMS (MALDI-TOF) calcd for $C_{78}H_{76}N_4O_6S_2Zn$ 1292.4492, found 1292.4489. UV–vis (THF) λ_{max} (log ε) 455 (5.56), 661 (4.84) nm. Fluorescence (THF, λ_{ex}=455 nm) λ_{em} 674 nm. IR (KBr) 2952, 2930, 2868, 2132, 2195, 1588, 1163 cm^{-1}.

4.2.5.2. Compound 1b. ^{1}H NMR (400 MHz, d_8-THF) δ 9.87 (d, J=5 Hz, 4H, β-pyrrole), 9.60 (d, J=5 Hz, 4H, β-pyrrole), 9.06 (d, J=5 Hz, 4H, β-pyrrole), 9.00 (d, J=5 Hz, 4H, β-pyrrole), 7.67 (d, J=8 Hz, 4H, Ar), 7.41 (d, J=8 Hz, 4H, Ar), 7.38 (d, J=2 Hz, 8H, Ar), 6.97 (t, J=2 Hz, 4H, Ar), 4.24 (t, J=6.6 Hz, 16H, OCH_2), 4.18 (s, 4H, SCH_2Ph), 2.34 (s, 6H, $C(O)CH_3$), 1.92 (sext, J=6.6 Hz, 16H, CH_2), 1.77 (m, J=6.6 Hz, 8H, CH), 1.01 (d, J=6.6 Hz, 48H, CH_3). HRMS (MALDI-TOF) calcd for $C_{134}H_{134}N_8O_{10}S_2Zn_2$ 2206.8241, found 2206.8234. UV–vis (THF) λ_{max} (log ε) 462 (5.50), 493 (4.95), 583 (4.19), 677 (4.82), 725 (4.75) nm. Fluorescence (THF, λ_{ex}=462 nm) λ_{em} 752 nm. IR (KBr) 2954, 2927, 2869, 2130, 2194, 1589, 1163 cm^{-1}.

4.2.5.3. Compound 1c. ^{1}H NMR (400 MHz, d_8-THF) δ 9.88 (m, 8H, β-pyrrole), 9.60 (d, J=5 Hz, 4H, β-pyrrole), 9.08 (m, 8H, β-pyrrole), 9.00 (d, J=5 Hz, 4H, β-pyrrole), 7.67 (d, J=8 Hz, 4H, Ar), 7.41 (d, 4H, Ar), 7.38 (m, 12H, Ar), 6.97 (m, 6H, Ar), 4.24 (m, 24H, OCH_2), 4.19 (s, 4H, SCH_2Ph), 2.35 (s, 6H, $C(O)CH_3$), 1.92 (m, 24H, CH_2), 1.77 (m, 12H, CH), 1.02 (m, 72H, CH_3). HRMS (MALDI-TOF) calcd for $C_{190}H_{192}N_{12}O_{14}S_2Zn_3$ 3121.1991, found 3121.2266. UV–vis (THF) λ_{max} (log ε) 463 (5.56), 583 (4.29), 744 (5.03) nm. Fluorescence (THF, λ_{ex}=463 nm) λ_{em} 786 nm. IR (KBr) 2954, 2927, 2868, 2129, 2162, 1590, 1156 cm^{-1}.

4.2.5.4. Compound 1d. ^{1}H NMR (400 MHz, d_8-THF) δ 9.88 (m, 12H, β-pyrrole), 9.60 (d, J=5 Hz, 4H, β-pyrrole), 9.08 (m, 12H, β-pyrrole), 9.00 (d, J=5 Hz, 4H, β-pyrrole), 7.67 (d, J=8 Hz, 4H, Ar), 7.41 (d, 4H, Ar), 7.38–7.44 (m, 16H, Ar), 6.97 (m, 8H, Ar), 4.24 (m, 32H, OCH_2), 4.19 (s, 4H, SCH_2Ph), 2.35 (s, 6H, $C(O)CH_3$), 1.92 (m, 32H, CH_2), 1.77 (m, 16H, CH), 1.02 (m, 96H, CH_3). MS (MALDI-TOF) calcd for $C_{246}H_{250}N_{16}O_{18}S_2Zn_4$ 4041.7, found 4041.5. UV–vis (THF) λ_{max} (log ε) 463 (5.70), 584 (4.43), 752 (5.24) nm. Fluorescence (THF, λ_{ex}=463 nm) λ_{em} 800 nm. IR (KBr) 2953, 2927, 2869, 2128, 2162, 1588, 1163 cm^{-1}.

4.2.5.5. Compound 1e. ^{1}H NMR (400 MHz, d_8-THF) δ 9.88 (m, 16H, β-pyrrole), 9.60 (d, J=5 Hz, 4H, β-pyrrole), 9.08 (m, 16H, β-pyrrole), 9.00 (d, J=5 Hz, 4H, β-pyrrole), 7.67 (d, J=8 Hz, 4H, Ar), 7.41 (d, 4H, Ar), 7.38–7.44 (m, 20H, Ar), 6.97 (m, 10H, Ar), 4.24 (m, 40H, OCH_2), 4.19 (s, 4H, SCH_2Ph), 2.35 (s, 6H, $C(O)CH_3$), 1.92 (m, 40H, CH_2), 1.77 (m, 20H, CH), 1.02 (m, 120H, CH_3). MS (MALDI-TOF) calcd for $C_{302}H_{308}N_{20}O_{22}S_2Zn_5$ 4964, found 4960. UV–vis (THF) λ_{max} (log ε) 463 (5.88), 585 (4.63), 758 (5.46) nm. Fluorescence (THF, λ_{ex}=463 nm) λ_{em} 814 nm. IR (KBr) 2953, 2926, 2868, 2128, 2162, 1588, 1162 cm^{-1}.

4.2.5.6. Compound 1f. ^{1}H NMR (400 MHz, d_8-THF) δ 9.88 (m, 20H, β-pyrrole), 9.60 (d, J=5 Hz, 4H, β-pyrrole), 9.08 (m, 20H, β-pyrrole), 9.00 (d, J=5 Hz, 4H, β-pyrrole), 7.67 (d, J=8 Hz, 4H, Ar), 7.41 (d, 4H, Ar), 7.38–7.44 (m, 24H, Ar), 6.97 (m, 12H, Ar), 4.24 (m, 48H, OCH_2), 4.19 (s, 4H, SCH_2Ph), 2.35 (s, 6H, $C(O)CH_3$), 1.92 (m, 48H, CH_2), 1.77 (m, 24H, CH), 1.02 (m, 144H, CH_3). MS (MALDI-TOF) calcd for $C_{358}H_{366}N_{24}O_{26}S_2Zn_6$ 5881, found 5876. UV–vis (THF) λ_{max} (log ε) 463 (5.97), 585 (4.81), 764 (5.56) nm. Fluorescence (THF, λ_{ex}=463 nm) λ_{em} 816 nm. IR (KBr) 2954, 2926, 2868, 2126, 2162, 1588, 1163 cm^{-1}.

4.2.5.7. Compound 1g. ^{1}H NMR (400 MHz, d_8-THF) δ 9.88 (m, 24H, β-pyrrole), 9.60 (d, J=5 Hz, 4H, β-pyrrole), 9.08 (m, 24H, β-pyrrole), 9.00 (d, J=5 Hz, 4H, β-pyrrole), 7.67 (d, J=8 Hz, 4H, Ar), 7.41 (d, 4H, Ar), 7.38–7.44 (m, 28H, Ar), 6.97 (m, 14H, Ar), 4.24 (m, 56H, OCH_2), 4.19 (s, 4H, SCH_2Ph), 2.35 (s, 6H, $C(O)CH_3$), 1.92 (m, 56H, CH_2), 1.77 (m, 28H, CH), 1.02 (m, 168H, CH_3). MS (MALDI-TOF) calcd for $C_{414}H_{424}N_{28}O_{30}S_2Zn_7$ 6799, found 6792. UV–vis (THF) λ_{max} (log ε) 463 (6.01), 585 (4.72), 768 (5.61) nm. Fluorescence (THF, λ_{ex}=463 nm) λ_{em} 816 nm. IR (KBr) 2953, 2927, 2869, 2121, 2166, 1588, 1162 cm^{-1}.

4.2.5.8. Compound 2a. ^{1}H NMR (400 MHz, d_8-THF) δ 9.57 (d, J=5 Hz, 4H, β-pyrrole), 9.02 (d, J=5 Hz, 4H, β-pyrrole), 8.83 (d, J=9 Hz, 2H, pyrene), 8.42–8.05 (16H, m, pyrene), 7.38 (d, J=2 Hz, 4H, Ar), 6.98 (t, J=2 Hz, 2H, Ar), 4.23 (t, J=7 Hz, 8H, OCH_2), 1.94 (sext, J=7 Hz, 8H, CH_2), 1.79 (m, J=7 Hz, 4H, CH), 1.01 (d, J=7 Hz, 24H,

CH_3). HRMS (MALDI-TOF) calcd for $C_{92}H_{76}N_4O_4Zn$ 1364.5152, found 1364.5150. UV–vis (THF) λ_{max} (log ε) 467 (5.47), 671 (4.88) nm. Fluorescence (THF, λ_{ex}=467 nm) λ_{em} 688 nm. IR (KBr) 2952, 2927, 2870, 2127, 2184, 1587, 1163 cm^{-1}.

4.2.5.9. Compound 2b. ^1H NMR (400 MHz, d_8-THF) δ 9.88 (d, J=5 Hz, 4H, β-pyrrole), 9.72 (d, J=5 Hz, 4H, β-pyrrole), 9.08 (d, J=5 Hz, 4H, β-pyrrole), 9.05 (d, J=5 Hz, 4H, β-pyrrole), 8.86 (d, J=9 Hz, 2H, pyrene), 8.44–8.06 (m, 16H, pyrene), 7.40 (d, J=2 Hz, 8H, Ar), 6.99 (t, J=2 Hz, 4H, Ar), 4.25 (t, J=7 Hz, 16H, OCH_2), 1.94 (sext, J=7 Hz, 16H, CH_2), 1.80 (m, J=7 Hz, 8H, CH), 1.02 (d, J=7 Hz, 48H, CH_3). HRMS (MALDI-TOF) calcd for $C_{148}H_{134}N_8O_8Zn_2$ 2278.8902, found 2278.8881. UV–vis (THF) λ_{max} (log ε) 468 (5.42), 580 (4.18), 685 (4.86), 730 (4.79) nm. Fluorescence (THF, λ_{ex}=468 nm) λ_{em} 758 nm. IR (KBr) 2953, 2927, 2869, 2127, 2184, 1588, 1164 cm^{-1}.

4.2.5.10. Compound 2c. ^1H NMR (400 MHz, d_8-THF) δ 9.91 (m, 8H, β-pyrrole), 9.73 (d, J=5 Hz, 4H, β-pyrrole), 9.10 (m, 8H, β-pyrrole), 9.05 (d, J=5 Hz, 4H, β-pyrrole), 8.86 (d, J=9 Hz, 2H, pyrene), 8.44–8.00 (m, 16H, pyrene), 7.42 (m, 12H, Ar), 6.99 (m, 6H, Ar), 4.25 (m, 24H, OCH_2), 1.96 (m, 24H, CH_2), 1.82 (m, 12H, CH), 1.03 (m, 72H, CH_3). HRMS (MALDI-TOF) calcd for $C_{204}H_{192}N_{12}O_{12}Zn_3$ 3193.2651, found 3193.2678. UV–vis (THF) λ_{max} (log ε) 468 (5.56), 584 (4.35), 747 (5.07) nm. Fluorescence (THF, λ_{ex}=468 nm) λ_{em} 782 nm. IR (KBr) 2954, 2928, 2868, 2125, 2167, 1587, 1162 cm^{-1}.

4.2.5.11. Compound 2d. ^1H NMR (400 MHz, d_8-THF) δ 9.91 (m, 12H, β-pyrrole), 9.73 (d, J=5 Hz, 4H, β-pyrrole), 9.10 (m, 12H, β-pyrrole), 9.05 (d, J=5 Hz, 4H, β-pyrrole), 8.86 (d, J=9 Hz, 2H, pyrene), 8.45–8.00 (m, 16H, pyrene), 7.42 (m, 16H, Ar), 6.99 (m, 8H, Ar), 4.26 (m, 32H, OCH_2), 1.96 (m, 32H, CH_2), 1.82 (m, 16H, CH), 1.03 (m, 96H, CH_3). MS (MALDI-TOF) calcd for $C_{260}H_{250}N_{16}O_{16}Zn_4$ 4117, found 4116. UV–vis (THF) λ_{max} (log ε) 469 (5.66), 584 (4.37), 756 (5.24) nm. Fluorescence (THF, λ_{ex}=469 nm) λ_{em} 796 nm. IR (KBr) 2954, 2925, 2869, 2126, 2167, 1588, 1163 cm^{-1}.

4.2.5.12. Compound 2e. ^1H NMR (400 MHz, d_8-THF) δ 9.91 (m, 16H, β-pyrrole), 9.73 (d, J=5 Hz, 4H, β-pyrrole), 9.10 (m, 16H, β-pyrrole), 9.05 (d, J=5 Hz, 4H, β-pyrrole), 8.86 (d, J=9 Hz, 2H, pyrene), 8.45–8.00 (m, 16H, pyrene), 7.42 (m, 20H, Ar), 6.99 (m, 10H, Ar), 4.26 (m, 40H, OCH_2), 1.96 (m, 40H, CH_2), 1.82 (m, 20H, CH), 1.03 (m, 120H, CH_3). MS (MALDI-TOF) calcd for $C_{316}H_{308}N_{20}O_{20}Zn_5$ 5034, found 5031. UV–vis (THF) λ_{max} (log ε) 469 (5.84), 584 (4.55), 762 (5.43) nm. Fluorescence (THF, λ_{ex}=469 nm) λ_{em} 802 nm. IR (KBr) 2951, 2927, 2870, 2126, 2167, 1588, 1162 cm^{-1}.

4.2.5.13. Compound 2f. ^1H NMR (400 MHz, d_8-THF) δ 9.91 (m, 20H, β-pyrrole), 9.73 (d, J=5 Hz, 4H, β-pyrrole), 9.10 (m, 20H, β-pyrrole), 9.05 (d, J=5 Hz, 4H, β-pyrrole), 8.86 (d, J=9 Hz, 2H, pyrene), 8.45–8.00 (m, 16H, pyrene), 7.42 (m, 24H, Ar), 6.99 (m, 12H, Ar), 4.26 (m, 48H, OCH_2), 1.96 (m, 48H, CH_2), 1.82 (m, 24H, CH), 1.03 (m, 144H, CH_3). MS (MALDI-TOF) calcd for $C_{372}H_{366}N_{24}O_{24}Zn_6$ 5953, found 5948. UV–vis (THF) λ_{max} (log ε) 469 (5.88), 584 (4.71), 766 (5.49) nm. Fluorescence (THF, λ_{ex}=469 nm) λ_{em} 806 nm. IR (KBr) 2956, 2927, 2869, 2126, 2162, 1588, 1163 cm^{-1}.

4.2.5.14. Compound 2g. ^1H NMR (400 MHz, d_8-THF) δ 9.91 (m, 24H, β-pyrrole), 9.73 (d, J=5 Hz, 4H, β-pyrrole), 9.10 (m, 24H, β-pyrrole), 9.05 (d, J=5 Hz, 4H, β-pyrrole), 8.86 (d, J=9 Hz, 2H, pyrene), 8.45–8.00 (m, 16H, pyrene), 7.42 (m, 28H, Ar), 6.99 (m, 14H, Ar), 4.26 (m, 56H, OCH_2), 1.96 (m, 56H, CH_2), 1.82 (m, 28H, CH), 1.03 (m, 168H, CH_3). MS (MALDI-TOF) calcd for $C_{428}H_{424}N_{28}O_{28}Zn_7$ 6868, found 6861. UV–vis (THF) λ_{max} (log ε) 469 (5.97), 583 (4.78), 769 (5.59) nm. Fluorescence (THF, λ_{ex}=469 nm) λ_{em} 808 nm. IR (KBr) 2954, 2927, 2869, 2126, 2162, 1588, 1163 cm^{-1}.

Acknowledgments

This work was supported by a Grant-in-Aid for Scientific Research (No. 15201028 and No. 14654135) from the Ministry of Culture, Education, Science, Sports, and Technology of Japan. The authors thank Professor T. Tsukuda of the Institute for Molecular Science for fluorescence measurements. One of the authors (H.T.) thanks Visionarts Inc. for financial support.

References and notes

1. Reed, M. A.; Lee, T. *Molecular Nanoelectronics*; American Scientific: Los Angeles, CA, 2003.
2. Flatt, A. K.; Dirk, S. M.; Henderson, J. C.; Shen, D. E.; Su, J.; Reed, M. A.; Tour, J. M. *Tetrahedron* **2003**, *59*, 8555–8570.
3. Tour, J. M.; Rawlett, A. M.; Kozaki, M.; Yao, Y. X.; Jagessar, R. C.; Dirk, S. M.; Price, D. W.; Reed, M. A.; Zhou, C. W.; Chen, J.; Wang, W. Y.; Campbell, I. *Chem. Eur. J.* **2001**, *7*, 5118–5134.
4. Reed, M. A. *Proc. IEEE* **1999**, *87*, 652–658.
5. Donhauser, Z. J.; Mantooth, B. A.; Kelly, K. F.; Bumm, L. A.; Monnell, J. D.; Stapleton, J. J.; Price, D. W.; Rawlett, A. M.; Allara, D. L.; Tour, J. M.; Weiss, P. S. *Science* **2001**, *292*, 2303–2307.
6. Blum, A. S.; Kushmerick, J. G.; Long, D. P.; Patterson, C. H.; Yang, J. C.; Henderson, J. C.; Yao, Y. X.; Tour, J. M.; Shashidhar, R.; Ratna, B. R. *Nat. Mater.* **2005**, *4*, 167–172.
7. Kubatkin, S.; Danilov, A.; Hjort, M.; Cornil, J.; Bredas, J. L.; Stuhr-Hansen, N.; Hedegard, P.; Bjornholm, T. *Nature* **2003**, *425*, 698–701.
8. Park, J.; Pasupathy, A. N.; Goldsmith, J. I.; Chang, C.; Yaish, Y.; Rinkoski, M.; Sethna, J. P.; Abruna, H. D.; McEuen, P. L.; Ralpa, D. C. *Nature* **2002**, *417*, 722–725.
9. Park, H.; Park, J.; Lim, A. K. L.; Anderson, E. H.; Alivisatos, A. P.; McEuen, P. L. *Nature* **2000**, *407*, 57–60.
10. Xu, B. Q.; Xiao, X. Y.; Yang, X. M.; Zang, L.; Tao, N. J. *J. Am. Chem. Soc.* **2005**, *127*, 2386–2387.
11. Liang, W. J.; Shores, M. P.; Bockrath, M.; Long, J. R.; Park, H. *Nature* **2002**, *417*, 725–729.
12. Chi, L. F.; Hartig, M.; Drechsler, T.; Schwaack, T.; Seidel, C.; Fuchs, H.; Schmid, G. *Appl. Phys. A* **1998**, *66*, S187–S190.
13. Brust, M.; Bethell, D.; Schiffrin, D. J.; Kiely, C. J. *Adv. Mater.* **1995**, *7*, 795–797.

14. Mbindyo, J. K. N.; Mallouk, T. E.; Mattzela, J. B.; Kratochvilova, I.; Razavi, B.; Jackson, T. N.; Mayer, T. S. *J. Am. Chem. Soc.* **2002**, *124*, 4020–4026.
15. Thess, A.; Lee, R.; Nikolaev, P.; Dai, H. J.; Petit, P.; Robert, J.; Xu, C. H.; Lee, Y. H.; Kim, S. G.; Rinzler, A. G.; Colbert, D. T.; Scuseria, G. E.; Tomanek, D.; Fischer, J. E.; Smalley, R. E. *Science* **1996**, *273*, 483–487.
16. Ebbesen, T. W.; Lezec, H. J.; Hiura, H.; Bennett, J. W.; Ghaemi, H. F.; Thio, T. *Nature* **1996**, *382*, 54–56.
17. Nuzzo, R. G.; Zegarski, B. R.; Dubois, L. H. *J. Am. Chem. Soc.* **1987**, *109*, 733–740.
18. Chen, R. J.; Zhang, Y. G.; Wang, D. W.; Dai, H. *J. Am. Chem. Soc.* **2001**, *123*, 3838–3839.
19. Ogawa, T.; Kobayashi, K.; Masuda, G.; Takase, T.; Maeda, S. *Thin Solid Films* **2001**, *393*, 374–378.
20. Huang, W.; Masuda, G.; Maeda, S.; Tanaka, H.; Ogawa, T. *Chem. Eur. J.* **2006**, *12*, 607–619.
21. Tanaka, H.; Yajima, T.; Matsumoto, T.; Ogawa, T. *Adv. Mater.*, in press.
22. Tanaka, H.; Yajima, T.; Masahiro, K.; Ogawa, T. *J. Nanosci. Nanotechnol.*, in press.
23. Taylor, P. N.; Huuskonen, J.; Rumbles, G.; Aplin, R. T.; Williams, E.; Anderson, H. L. *Chem. Commun.* **1998**, 909–910.
24. Screen, T. E. O.; Thorne, J. R. G.; Denning, R. G.; Bucknall, D. G.; Anderson, H. L. *J. Mater. Chem.* **2003**, *13*, 2796–2808.
25. Seybold, P. G.; Gouterman, M. *J. Mol. Spectrosc.* **1969**, *31*, 1–13.
26. Kim, Y. H.; Jeong, D. H.; Kim, D.; Jeoung, S. C.; Cho, H. S.; Kim, S. K.; Aratani, N.; Osuka, A. *J. Am. Chem. Soc.* **2001**, *123*, 76–86.
27. Ogawa, T.; Nishimoto, Y.; Yoshida, N.; Ono, N.; Osuka, A. *Angew. Chem., Int. Ed.* **1999**, *38*, 176–179.
28. Ogawa, T.; Nishimoto, Y.; Yoshida, N.; Ono, N.; Osuka, A. *Chem. Commun.* **1998**, 337–338.
29. Kawao, M.; Ozawa, H.; Tanaka, H.; Ogawa, T. *Thin Solid Films* **2006**, *499*, 23–28.
30. Plater, M. J.; Aiken, S.; Bourhill, G. *Tetrahedron* **2002**, *58*, 2405–2413.
31. Gryko, D. T.; Clausen, C.; Roth, K. M.; Dontha, N.; Bocian, D. F.; Kuhr, W. G.; Lindsey, J. S. *J. Org. Chem.* **2000**, *65*, 7345–7533.
32. Hissler, M.; Harriman, A.; Khatyr, A.; Ziessel, R. *Chem. Eur. J.* **1999**, *5*, 3366–3381.